Bis(tertiary phosphine)palladium(0) and -platinum(0) Complexes: Preparations and Crystal and Molecular Structures

S. Otsuka,*[1a] T. Yoshida,[1a] M. Matsumoto,[1b] and K. Nakatsu[1b]

Contribution from the Department of Chemistry, Faculty of Engineering Science, Osaka University, Toyonaka, Osaka, Japan 560, and Faculty of Science, Kwansei Gakuin University, Nishinomiya, Hyogo, Japan 662.

Received November 3, 1975

Abstract: Discrete linear complexes of PdL_2 (**1**, L = $P(t\text{-Bu})_3$; **2**, $PPh(t\text{-Bu})_2$; **3**, $P(c\text{-}C_6H_{11})_3$) were prepared from $Pd(\eta^5\text{-}C_5H_5)(\eta^3\text{-}C_3H_5)$, and analogous PtL_2 (**4**, L = $P(t\text{-Bu})_3$; **5**, $PPh(t\text{-Bu})_2$; **6**, $P(c\text{-}C_6H_{11})_3$; **7**, $P(i\text{-Pr})_3$) from *trans*-$PtCl_2L_2$ or $Pt(COD)_2$. These were characterized by inter alia mass and ^1H NMR spectra. The crystal and molecular structures of **2** and **5** were determined by three-dimensional x-ray structural analysis. Crystals of both are orthorhombic, space group *Fdd*2 ($C_{2v}{}^{19}$) with a = 45.377 (7) Å, b = 12.628 (2) Å, c = 10.070 (2) Å, and Z = 8 for **2**, and a = 45.100 (4) Å, b = 12.590 (1) Å, c = 10.048 (1) Å, and Z = 8 for **5**. The weighted and unweighted R values for **2** were 0.060 and 0.054, respectively (for 1644 reflections), while the corresponding R values for **5** were 0.034 and 0.033 (for 1973 reflections). Both molecules have C_2 crystallographic symmetry. The metal atom assumes a slightly bent linear coordination with a P–Pd–P angle of 176.6 (1)° and a P–Pt–P angle of 177.0 (1)°. The substituents of the phosphorus atoms form an eclipsed conformation with nearly parallel phenyl planes. The M–P distances are 2.285 (2) Å for **2** and 2.252 (1) Å for **5**. The nonbonded metal···ortho-hydrogen atom distance is estimated to be 2.83 Å for both complexes, while the distance between two ortho-hydrogen atoms is ca. 2.6 Å in **2** and 2.5 Å in **5**. The shortest aliphatic hydrogen atom···metal distance is 2.70 Å. Reduction of *trans*-$PtCl_2[P(i\text{-Pr})_3]_2$ in the presence of $P(i\text{-Pr})_3$ gives $Pt[P(i\text{-Pr})_3]_3$ (**8**) which tends to dissociate affording **7**. No indication was obtained for the formation of ML_3 with $PPh(t\text{-Bu})_2$ or $P(t\text{-Bu})_3$. Factors governing the coordination number are discussed in terms of steric and electronic effects.

Two coordinate phosphine complexes of the zerovalent platinum triad have received considerable interest. Dissociation of $M(PPh_3)_4$ (M = Pd, Pt) to give $M(PPh_3)_n$ (n = 3, 2, 1) has been postulated to account for the very low molecular weight of $M(PPh_3)_4$.[2] Their existence as intermediates was postulated in substitution reactions of PtL_2L' (L = PR_3, L′ = acetylene, PR_3).[3] There is poor information on the elusive species $Pt(PPh_3)_2$;[4] it appears to have a strong propensity to form polynuclear compounds[5] such as $[Pt(PPh_3)_3]_2$ or $[Pt(PPh_3)_2]_3$. Recently a few ML_2 complexes of Ni(0),[6-8] Pd(0),[9-13] and Pt(0)[14,15] (L = $P(c\text{-}C_6H_{11})_3$, $P(i\text{-Pr})_3$, $PPh(t\text{-Bu})_2$, $P(t\text{-Bu})_3$, $P(O\text{-}o\text{-}C_6H_4C_6H_5)_3$, $P(O\text{-}(+)\text{-borna-2-yl})_3$) have been reported.

Obviously, low coordination can be stabilized by ligand bulk, as exemplified by the existence of the unusual compounds $M[N(SiMe_3)_2]_n$ (M = Fe,[16] Co,[17] etc.; n = 3, 2). The existence of a few stable ML_2 complexes (M = Pd, Pt; L = bulky phosphines or phosphites) also indicates the paramount importance of steric factors. However, the role of electronic factors in governing the coordination number and the stability of such complexes are not fully understood. For this reason structural information on such complexes is desirable. This paper describes the molecular structures of PdL_2 and PtL_2 for L = $PPh(t\text{-Bu})_2$ and general preparative routes for ML_2 complexes with a variety of phosphines. Some of these complexes are exceedingly reactive and show a very rich chemistry which will be described separately.

Experimental Section

^1H NMR spectra were recorded on a 100-MHz Model JNM 4H-100 (JEOL) NMR spectrometer, ir spectra on a Hitachi Perkin-Elmer Model 225 ir spectrometer, and mass spectra on JMS-D100(JEOL) mass spectrometer. All reactions and physical measurements were carried out in a nitrogen atmosphere. The following reagents were prepared according to known methods: $P(t\text{-Bu})_3$,[18] $PPh(t\text{-Bu})_2$,[19] $P(c\text{-}C_6H_{11})_3$,[20] $P(i\text{-Pr})_3$,[21] $P(O\text{-}o\text{-}C_6H_4CH_3)_3$,[22] $Pd(\eta^5\text{-}C_5H_5)(\eta^3\text{-}C_3H_5)$,[23] $Pt(COD)_2$[15] (COD = 1,5-cyclooctadiene), and *trans*-$PtCl_2[PPh(t\text{-Bu})_2]_2$.[19] The following *trans*-$PtCl_2L_2$ complexes were prepared similarly:[19] *trans*-$PtCl_2[P(i\text{-Pr})_3]_2$ ($\nu_{(Pt-Cl)}$ 333 cm^{-1}; δ 1.38 (q (CH_3), $^3J_{H-P} + {}^5J_{H-P}$ = 14.0 Hz, J_{H-H} = 7.0 Hz) and 2.96 (m (CH)); mp 256–265°. Anal. Calcd for $C_{18}H_{42}Cl_2P_2Pt$: C, 36.85; H, 7.22. Found: C, 36.63; H, 7.18) and *trans*-$PtCl_2[P(c\text{-}C_6H_{11})_3]_2$ ($\nu_{(Pt-Cl)}$ 335 cm^{-1}; mp >300°. Anal. Calcd for $C_{36}H_{66}Cl_2P_2Pt$: C, 52.28; H, 8.04. Found: C, 51.87; H, 7.95).

I. Preparation. $Pd[P(t\text{-Bu})_3]_2$ (1). A mixture of $Pd(\eta^5\text{-}C_5H_5)(\eta^3\text{-}C_3H_5)$ (0.21 g, 1 mmol) and $P(t\text{-Bu})_3$ (0.60 g, 3 mmol) in n-hexane (10 ml) was stirred at room temperature for 3 h. The pale red mixture was filtered and concentrated in vacuo to about a half volume; the concentrate was kept at −20° for 3 h to give **1** as colorless crystals. Recrystallization from n-hexane gave an analytically pure sample (0.3 g, 60%), mp 160–163° dec. Anal. Calcd for $C_{24}H_{54}P_2Pd$: C, 56.40; H, 10.67; mol wt, 510. Found: C, 56.62; H, 10.73; mol wt, 484 (benzene).

$Pd[PPh(t\text{-Bu})_2]_2$ (2). This complex was obtained, following the same procedure employing $PPh(t\text{-Bu})_2$, as colorless crystals (60%), mp 122–126° dec. Anal. Calcd for $C_{28}H_{46}P_2Pd$: C, 61.01; H, 8.41; mol wt, 550. Found: C, 60.81; H, 8.46; mol wt, 470 (benzene).

$Pd[P(c\text{-}C_6H_{11})_3]_2$ (3). A similar reaction with $P(c\text{-}C_6H_{11})_3$ in benzene (40–45°, 15 h) gave **3** as colorless crystals (62%) after recrystallization from toluene, mp 102–104° dec. Anal. Calcd for $C_{36}H_{66}P_2Pd$: C, 64.79; H, 9.99. Found: C, 64.76; H, 9.97.

$Pt[P(t\text{-Bu})_3]_2$ (4). A mixture of $Pt(COD)_2$ (0.10 g, 0.25 mmol) and $P(t\text{-Bu})_3$ (0.13 g, 0.6 mmol) in n-hexane (10 ml) was stirred at room temperature for 5 h. The mixture was filtered and concentrated to give colorless crystals (0.08 g, 54%), which were recrystallized from n-hexane, mp 234–238° dec. Anal. Calcd for $C_{24}H_{54}P_2Pt$: C, 48.05; H, 9.07; mol wt, 599. Found: C, 48.77; H, 9.10; mol wt, 599 (mass).

$Pt[PPh(t\text{-Bu})_2]_2$ (5). Reduction of *trans*-$PtCl_2[PPh(t\text{-Bu})_2]_2$ (1.00 g, 1.41 mmol) with 1% Na/Hg (23 g) in THF (20 ml) at room temperature gave a solid product after usual workup. The solid was recrystallized from hexane to give **5** as colorless crystals (0.80 g, 88%), mp 160–162° dec. Anal. Calcd for $C_{28}H_{46}P_2Pt$: C, 52.57; H, 9.25; mol wt, 639. Found: C, 51.98; H, 7.35; mol wt, 620 (benzene), 639 (mass).

$Pt[P(c\text{-}C_6H_{11})_3]_2$ (6). A similar reduction of *trans*-$PtCl_2[P(c\text{-}C_6H_{11})_3]_2$ with 1% Na/Hg gave **6** as colorless crystals (50%). Alternatively, *trans*-$PtCl_2[P(c\text{-}C_6H_{11})_3]_2$ (1.65 g, 2 mmol) was reduced with a THF (10 mmol) solution of sodium naphthalenide at room temperature for 5 h. The dark brown residue obtained on concentration was extracted with n-hexane. After evaporation, naphthalene was removed from the pale brown residue by sublimation at 40–50 °C under vacuum. Recrystallization of the residue from a toluene–n-

hexane mixture gave **6** (0.81 g, 52%), mp 115–118° dec. Anal. Calcd for $C_{36}H_{66}P_2Pt$: C, 57.19; H, 8.80; mol wt, 755. Found: C, 57.11; H, 8.98; mol wt, 755 (mass).

$Pt[P(\textit{i}\text{-}Pr)_3]_2$ (7). A similar reduction of *trans*-$PtCl_2[P(\textit{i}\text{-}Pr)_3]_2$ (0.58 g, 1 mmol) with 1% Na/Hg (12 g) gave crude pale yellow crystals of **7**. Recrystallization to obtain an analytical sample was unsuccessful. Alternatively, sublimation of $Pt[P(\textit{i}\text{-}Pr)_3]_3$ (**8**) (vide infra) at 50–60 °C under high vacuum (10^{-4} mmHg) gave low-melting crystals, which were identified by the mass and ^1H NMR spectra as **7**.

$Pt[P(\textit{i}\text{-}Pr)_3]_3$ (8). A similar reduction (16 h, 20–30 °C) of a mixture of *trans*-$PtCl_2[P(\textit{i}\text{-}Pr)_3]_2$ (1.00 g, 1.72 mmol) and $P(\textit{i}\text{-}Pr)_3$ (0.28 g, 1.80 mmol) with 1% Na/Hg (23 g) in THF (10 ml) gave a pale yellow solid. Recrystallization from pentane at −50 °C gave **8** as pale yellow crystals (0.70 g, 60%) which had the characteristic odor of free $P(\textit{i}\text{-}Pr)_3$. Anal. Calcd for $C_{27}H_{63}P_3Pt$: C, 47.97; H, 9.39; mol wt, 675. Found: C, 46.66; H, 8.91; mol wt, 352 (benzene).

$Pt[P(O\text{-}\textit{o}\text{-}C_6H_4CH_3)_3]_3$ (9). From a mixture of $Pt(COD)_2$ (0.06 g, 0.15 mmol) and $P(O\text{-}\textit{o}\text{-}C_6H_4CH_3)_3$ (0.15 g, 0.45 mmol) in *n*-hexane (7 ml) stirred for 3 h was obtained pale yellow crystals which were recrystallized from a toluene-*n*-hexane mixture (0.10 g, 53%), mp 176–177 °C. Anal. Calcd for $C_{63}H_{63}O_9P_3Pt$: C, 60.42; H, 5.07; mol wt, 1252. Found: C, 60.48; H, 5.13; mol wt, 1259 (benzene). Treatment of **9** with 3 mol of $P(O\text{-}\textit{o}\text{-}C_6H_4CH_3)_3$ in benzene at room temperature merely resulted in a complete recovery of **9**.

II. Collection and Reduction of X-Ray Data. Crystals of the two $PPh(\textit{t}\text{-}Bu)_2$ complexes **2** and **5** were grown from *n*-hexane solutions as very air sensitive, yellow prisms. Each specimen was sealed in a nitrogen-filled glass capillary tube to prevent oxidative decomposition. Oscillation and Weissenberg photographs of both crystals indicated orthorhombic lattices. The systematic absences, hkl for $h + k \neq 2n$ and $k + l \neq 2n$, $0kl$ for $k + l \neq 4n$, and $h0l$ for $h + l \neq 4n$, uniquely determined the space group as $Fdd2$ ($C_{2v}{}^{19}$) for both crystals. The space group Cc assigned previously[9] must be corrected. Accurate unit cell dimensions were obtained with Mo Kα radiation (λ 0.71069 Å) at 20 °C from the least-squares treatment of 2θ angles of reflections carefully measured on a Rigaku four-circle diffractometer: $a = 45.377$ (7), $b = 12.628$ (2), $c = 10.070$ (2) Å for **2** and $a = 45.100$ (4), $b = 12.590$ (1), $c = 10.048$ (1) Å for **5**. The 12 and 15 reflections ($31° < 2\theta < 41°$) were measured for **2** and **5**, respectively. The standard deviations are based on the least-squares calculation of the 2θ angles. The extreme air sensitivity of the complexes precluded an experimental density determination. The calculated density for eight complex molecules per unit cell is 1.268 g cm^{-3} for **2** and 1.489 g cm^{-3} for **5**. The complex molecules showed $2(C_2)$ crystallographic symmetry.

The intensity data for **2** were collected by the θ–2θ scan method on a Rigaku computer-controlled four-circle diffractometer using Zr-filtered Mo Kα radiation, the c axis being placed along the diffractometer ϕ axis, while those for **5** were obtained by the same method in a similar crystal orientation using monochromatized Mo Kα radiation from the (002) plane of a highly mosaic graphite crystals. One independent set of data was measured out to $2\theta = 55°$ for **2** and 60° for **5**. Since three monitoring reflections of **2** showed a regular, isotropic, time-dependent loss of intensity (10% during the entire data collection), the reflections were corrected as a function of exposure time. The corresponding loss for **5** being only 2%, no correction was necessary. Absorption corrections with 5000 grids were made for both complexes. Linear absorption coefficients were 7.57 and 50.9 cm^{-1} for **2** and **5**, respectively, and the transmission factors calculated were within a range 0.80 to 0.86 for **2** and 0.15 to 0.32 for **5**. The observed intensity for a reflection was calculated by $I_o = N - 0.5(b_1 + b_2)\cdot(t_c/t_b)$ and the standard deviation by $\sigma(F_o) = \frac{1}{2}[(N + 0.25(b_1 + b_2)(t_c/t_b)^2)/(\mathrm{Lp}) - (I_o)]^{1/2}$, where N is the total number of counts measured during a scan time t_c, and b_1 and b_2 are the number of background counts each obtained during a time t_b. The intensity data were reduced to the values of $|F_o|$, observed structure amplitudes. Of the 1741 reflections collected for **2** 1644 with $|F_o| > 3\sigma(F_o)$ were used as a basis for the subsequent structure analysis. For **5** the 1973 reflections of the 2201 collected were considered with the same criterion.

III. Solution and Refinement of the Structures. The structure of **2** was solved straightforwardly by the usual combination of Patterson, Fourier, and block-diagonal least-squares methods with one block for all parameters of each atom. In the least-squares calculations the function $\Sigma w(|F_o| - |F_c|)^2$ was minimized, where $|F_c|$ is the calculated structure amplitude and w is the weight (vide infra). The location of the metal atom was fixed arbitrarily at the origin throughout the refinement. The refinement of all the non-hydrogen atoms with individual anisotropic thermal factors has led to 0.060 and 0.076 for R and R_w, respectively. The agreement indices, R and R_w, are defined as $\Sigma||F_o| - |F_c||/\Sigma|F_o|$ and $[\Sigma w(||F_o| - |F_c||)^2]^{1/2}$, respectively. Since the two complexes were expected to be isomorphous, the refinement of **5** was initiated with the final coordinates of the non-hydrogen atoms of **2**. A similar refinement procedure resulted in convergence to $R = 0.040$ and $R_w = 0.042$.

Atomic scattering factors for Pt, Pd, P, and C were those calculated by Cromer and Waber[24] and the factor for H by Stewart et al.[25] The values of the anomalous dispersion terms, $\Delta f'$ and $\Delta f''$, for the Pt, Pd, and P atoms were taken from the tabulation of Cromer and Liberman[26] and included in the structure factor calculations.

All the hydrogen atoms of both complex molecules were revealed from difference Fourier maps; the phenyl hydrogen atoms were found from the general plane difference map through the phenyl ring and the methyl hydrogen atoms from the map through a plane 0.33 Å apart from the methyl carbon atom and vertical to the C–C bond. The peaks on the maps were in the range of 0.3–0.5 e/Å^3. Isotropic thermal vibrations were assumed for all the hydrogen atoms to refine their parameters. In the final refinement cycles for both complexes no individual parameter shift was greater than the corresponding estimated standard deviation. The weighting scheme $w = 1/(\sigma^2(F_o) + a|F_o|^2)$ was assumed, where the coefficient, a, was chosen to satisfy the equation, $\Sigma(|F_o| - |F_c|)^2 = \sigma^2(F_o) + a|F_o|^2$, so that the average values of $w(|F_o| - |F_c|)^2$ for several subgroups of increasing $|F_o|$'s were reasonably constant. In the last cycle of refinement, a was 0.0031 and 0.0014 for **2** and **5**, respectively. The final values of R and R_w are 0.054 and 0.060 for **2** and 0.033 and 0.034 for **5**, respectively.

Subsequent difference maps showed no unusual features; all the residual peaks for **2** were less than 0.3 e/Å^3, while 0.4 e/Å^3 for **5**.

All the numerical calculations were carried out on a FACOM 270-20 computer of Kwansei Gakuin University using the programs written in our laboratory.

The final positional and thermal parameters for the non-hydrogen atoms are given in Table I and II, and those for hydrogen atoms in Table III. The final values of the structure amplitudes are tabulated as $|F_o|$ and $|F_c|$ for those reflections used in the refinement.[27]

Results

Preparative Chemistry. Several two coordinate Pd(0) complexes, PdL_2 (**1**, L = $P(\textit{t}\text{-}Bu)_3$; **2**, L = $PPh(\textit{t}\text{-}Bu)_2$; **3**, $P(c\text{-}C_6H_{11})_3$), were prepared by treating $Pd(\eta^5\text{-}C_5H_5)(\eta^3\text{-}C_3H_5)$ with an appropriate phosphine in *n*-hexane or benzene. Platinum analogues PtL_2 (**5**, L = $PPh(\textit{t}\text{-}Bu)_2$; **6**, L = $P(c\text{-}C_6H_{11})_3$; **7**, L = $P(\textit{i}\text{-}Pr)_3$) were obtained simply by reducing the corresponding chloride *trans*-$PtCl_2L_2$ with Na/Hg (sodium amalgam) or sodium naphthalenide in THF at room temperature. A pale yellow three-coordinate complex $Pt[P(\textit{i}\text{-}Pr)_3]_3$ (**8**) can be prepared by adding 1 mol of $P(\textit{i}\text{-}Pr)_3$ in the reduction of *trans*-$PtCl_2[P(\textit{i}\text{-}Pr)_3]_2$. The complex **8** readily liberates 1 mol of $P(\textit{i}\text{-}Pr)_3$ at 50–60 °C under high vacuum affording colorless low-melting **7**. Although recrystallization of crude **7** to obtain an analytically pure sample failed, owing to its extraordinary solubility in hydrocarbons, low melting, and extreme air sensitivity, sublimation in vacuo produced a fairly pure sample, as revealed by its mass and ^1H NMR spectrum (vide infra).

$$Pd(\eta^5\text{-}C_5H_5)(\eta^3\text{-}C_3H_5) + 2L \rightarrow PdL_2 + \text{hydrocarbons} \quad (1)$$

$$\textit{trans}\text{-}PtCl_2L_2 \xrightarrow{\text{Na/Hg or NaC}_{10}\text{H}_8} PtL_2 + 2NaCl \quad (2)$$

$$L = \text{phosphine}$$

Preparation of $Pt[P(\textit{t}\text{-}Bu)_3]_2$ (**4**) by this method proved to be impossible since attempts to prepare *trans*-$PtCl_2[P(\textit{t}\text{-}Bu)_3]_2$ by treating K_2PtCl_4 with $P(\textit{t}\text{-}Bu)_3$ in an EtOH-H_2O mixture resulted in nearly complete reduction of Pt(II) to platinum metal together with a small amount of colorless crystals of

Table I. Final Fractional Positional Parameters for the Non-Hydrogen Atoms

	$Pd[PPh(t\text{-}Bu)_2]_2$			$Pt[PPh(t\text{-}Bu)_2]_2$		
Atom	*x*	*y*	*z*	*x*	*y*	*z*
Metal	0	0	0	0	0	0
P	0.045 83 (4)	0.0748 (2)	0.0068 (3)	0.045 61 (3)	0.0727 (1)	0.0060 (3)
C(1)	0.062 04 (17)	0.0930 (8)	−0.1573 (9)	0.061 41 (16)	0.0924 (6)	−0.1605 (7)
C(2)	0.091 15 (18)	0.1194 (10)	−0.1853 (10)	0.091 39 (17)	0.1175 (9)	−0.1876 (10)
C(3)	0.101 45 (21)	0.1224 (11)	−0.3146 (12)	0.101 75 (23)	0.1207 (10)	−0.3194 (12)
C(4)	0.082 86 (24)	0.1051 (10)	−0.4223 (11)	0.082 59 (24)	0.1025 (10)	−0.4233 (12)
C(5)	0.053 44 (23)	0.0842 (11)	−0.3965 (10)	0.053 32 (23)	0.0816 (9)	−0.3997 (10)
C(6)	0.043 29 (19)	0.0783 (8)	−0.2653 (11)	0.043 13 (20)	0.0758 (8)	−0.2685 (8)
C(7)	0.045 88 (19)	0.2108 (9)	0.0852 (10)	0.045 67 (19)	0.2107 (8)	0.0826 (10)
C(8)	0.022 78 (22)	0.2733 (8)	0.0049 (18)	0.021 95 (26)	0.2712 (8)	0.0043 (17)
C(9)	0.035 65 (28)	0.2057 (11)	0.2309 (14)	0.035 39 (28)	0.2016 (11)	0.2282 (12)
C(10)	0.074 55 (22)	0.2760 (10)	0.0745 (15)	0.074 96 (25)	0.2730 (9)	0.0756 (17)
C(11)	0.072 07 (19)	−0.0180 (9)	0.0944 (11)	0.072 12 (19)	−0.0202 (7)	0.0927 (11)
C(12)	0.076 78 (22)	−0.1107 (9)	−0.0049 (17)	0.076 57 (26)	−0.1134 (9)	−0.0059 (17)
C(13)	0.056 56 (24)	−0.0593 (12)	0.2196 (12)	0.056 40 (26)	−0.0651 (11)	0.2173 (11)
C(14)	0.101 95 (22)	0.0270 (11)	0.1389 (14)	0.103 00 (25)	0.0217 (10)	0.1344 (16)

Table II. Thermal Parameters[a] ($\times 10^4$) for the Non-Hydrogen Atoms

Atom	U_{11}	U_{22}	U_{33}	U_{12}	U_{23}	U_{13}
			(a) $Pd\ [PPh(t\text{-}Bu)_2]_2$			
Pd	229 (4)	655 (5)	403 (4)	−112 (4)	0	0
P	209 (10)	587 (12)	342 (10)	−61 (9)	71 (14)	−20 (10)
C(1)	303 (42)	630 (61)	358 (45)	−23 (41)	80 (46)	20 (35)
C(2)	303 (42)	1043 (86)	536 (59)	23 (52)	192 (64)	38 (42)
C(3)	407 (52)	1066 (92)	652 (69)	96 (60)	297 (72)	122 (50)
C(4)	709 (63)	866 (83)	455 (62)	64 (62)	125 (62)	196 (53)
C(5)	636 (63)	1191 (105)	317 (52)	−155 (67)	57 (64)	−89 (47)
C(6)	438 (42)	784 (68)	450 (59)	−112 (46)	44 (60)	24 (46)
C(7)	365 (42)	737 (66)	468 (54)	−144 (46)	−57 (52)	−16 (42)
C(8)	563 (52)	619 (65)	1221 (99)	19 (51)	−7 (92)	−9 (88)
C(9)	1033 (83)	1009 (95)	578 (88)	−145 (75)	−252 (77)	69 (72)
C(10)	459 (52)	802 (87)	1178 (106)	−205 (57)	−190 (82)	−41 (65)
C(11)	365 (42)	712 (75)	662 (65)	16 (46)	250 (61)	−37 (45)
C(12)	657 (63)	791 (76)	932 (86)	228 (57)	179 (96)	45 (88)
C(13)	605 (63)	1389 (117)	748 (91)	−165 (74)	624 (89)	−57 (59)
C(14)	396 (52)	1105 (105)	992 (95)	−65 (60)	379 (85)	−279 (57)
			(b) $Pt[PPh(t\text{-}Bu)_2]_2$			
Pt	247 (1)	454 (2)	307 (1)	−68 (1)	0	0
P	258 (10)	415 (7)	287 (7)	−49 (6)	61 (9)	−21 (8)
C(1)	371 (31)	435 (36)	224 (27)	−23 (27)	64 (27)	−36 (25)
C(2)	319 (31)	843 (63)	418 (45)	30 (37)	169 (47)	−53 (34)
C(3)	443 (52)	993 (80)	565 (59)	58 (49)	195 (62)	230 (44)
C(4)	701 (62)	714 (65)	495 (57)	52 (50)	128 (52)	222 (52)
C(5)	701 (62)	757 (63)	328 (42)	−30 (47)	2 (45)	−32 (42)
C(6)	526 (41)	694 (52)	250 (40)	−116 (39)	−3 (36)	−77 (31)
C(7)	433 (41)	492 (40)	467 (48)	−85 (36)	−72 (40)	11 (38)
C(8)	556 (52)	533 (43)	766 (77)	63 (42)	54 (56)	−103 (67)
C(9)	876 (82)	851 (81)	518 (70)	−190 (65)	−293 (62)	84 (56)
C(10)	484 (52)	627 (55)	928 (97)	−275 (43)	−9 (62)	−42 (60)
C(11)	371 (41)	552 (47)	466 (47)	−35 (30)	150 (38)	−102 (36)
C(12)	793 (72)	609 (59)	851 (92)	197 (47)	93 (78)	−93 (85)
C(13)	752 (72)	872 (80)	402 (49)	−83 (59)	281 (54)	−86 (45)
C(14)	422 (52)	971 (80)	838 (96)	−91 (49)	371 (71)	−278 (59)

[a] The thermal parameters are of the form $\exp[-2\pi^2(a^{*2}h^2U_{11}{}^2 + b^{*2}k^2U_{22}{}^2 + c^{*2}l^2U_{33} + 2a^*b^*hkU_{12} + 2b^*c^*klU_{23} + 2a^*c^*hlU_{13})]$.

composition $PtCl[P(t\text{-}Bu)_2C(CH_3)_2CH_2][P(t\text{-}Bu)_3]$. This material was not characterized further because of the extremely low yield. In contrast, a similar reaction of $P(t\text{-}Bu)_3$ with $Pd(PhCN)_2Cl_2$ gives unexpectedly a hydride complex *trans*-$PdH(Cl)[P(t\text{-}Bu)_3]_2$.[28] Complex **4** was successfully prepared by treating $Pt(COD)_2$ (COD = 1,5-cyclooctadiene) with $P(t\text{-}Bu)_3$ in hexane. This method has been employed for the preparation of $Pt[P(c\text{-}C_6H_{11})_3]_2$.[15]

$$Pt(\eta^4\text{-}COD)_2 + 2L \rightarrow PtL_2 + 2COD \qquad (3)$$

A similar reaction of $Pt(COD)_2$ with $P(O\text{-}o\text{-}C_6H_4CH_3)_3$ gave $Pt[P(O\text{-}o\text{-}C_6H_4CH_3)_3]_3$ (**9**); two-coordinate complex $Pt[P(O\text{-}o\text{-}C_6H_4CH_3)_3]_2$ could not be isolated from the reaction with 2 mol of the phosphite.

The two-coordinate complexes thus obtained are mostly colorless, diamagnetic crystals soluble in saturated hydrocarbons but insoluble in alcohol. Compounds **1** and **4** are stable in air in the solid state while **7** and **8** are extremely unstable. Compounds **2, 3, 5,** and **6** are stable in air for several minutes in the solid state. The pale yellow phosphite complex **9** is sol-

Table III. Fractional Positional and Isotropic Thermal[a] ($\times 10^2$, Å^2) Parameters for the Hydrogen Atoms

Atom[b]	x	y	z	U
		(a) $Pd[PPh(t\text{-}Bu)_2]_2$		
H[C(2)]	0.105 (2)	0.131 (8)	−0.112 (8)	6.0 (3.0)
H[C(3)]	0.122 (2)	0.139 (8)	−0.333 (9)	7.6 (3.5)
H[C(4)]	0.091 (2)	0.102 (8)	−0.513 (10)	8.9 (3.5)
H[C(5)]	0.040 (2)	0.073 (8)	−0.470 (10)	8.8 (3.5)
H[C(6)]	0.022 (2)	0.065 (7)	−0.249 (10)	8.7 (3.2)
H(1)[C(8)]	0.019 (2)	0.345 (8)	0.046 (8)	7.0 (3.4)
H(2)[C(8)]	0.005 (2)	0.234 (6)	−0.002 (10)	5.7 (2.6)
H(3)[C(8)]	0.029 (2)	0.287 (8)	−0.084 (9)	7.6 (3.4)
H(1)[C(9)]	0.051 (2)	0.174 (8)	−0.287 (10)	9.6 (3.5)
H(2)[C(9)]	0.019 (2)	0.158 (8)	0.240 (10)	10.2 (3.5)
H(3)[C(9)]	0.030 (1)	0.277 (5)	0.265 (8)	5.5 (2.5)
H(1)[C(10)]	0.071 (2)	0.353 (8)	0.105 (8)	6.9 (3.2)
H(2)[C(10)]	0.082 (2)	0.275 (7)	−0.017 (9)	7.0 (3.1)
H(3)[C(10)]	0.091 (2)	0.238 (8)	0.125 (9)	8.1 (3.5)
H(1)[C(12)]	0.086 (2)	−0.085 (7)	−0.087 (9)	6.9 (3.2)
H(2)[C(12)]	0.057 (2)	−0.143 (8)	−0.025 (9)	7.2 (3.3)
H(3)[C(12)]	0.090 (2)	−0.166 (8)	0.038 (9)	8.5 (3.5)
H(1)[C(13)[	0.064 (2)	−0.135 (8)	0.234 (10)	8.3 (3.4)
H(2)[C(13)]	0.035 (2)	−0.071 (8)	0.197 (9)	9.1 (3.5)
H(3)[C(13)]	0.059 (2)	−0.017 (8)	0.295 (8)	6.9 (3.2)
H(1)[C(14)]	0.111 (2)	0.070 (8)	0.068 (9)	8.3 (3.5)
H(2)[C(14)]	0.116 (2)	−0.026 (8)	0.158 (10)	9.6 (3.5)
H(3)[C(14)]	0.099 (2)	0.077 (8)	0.211 (9)	8.8 (3.5)
		(b) $Pt[PPh(t\text{-}Bu)_2]_2$		
H[C(2)]	0.105 (2)	0.131 (8)	−0.115 (10)	5.8 (3.1)
H[C(3)]	0.123 (2)	0.141 (8)	−0.335 (11)	6.7 (3.7)
H[C(4)]	0.091 (2)	0.104 (8)	−0.513 (13)	7.3 (3.6)
H[C(5)]	0.039 (2)	0.066 (9)	−0.473 (13)	6.4 (3.3)
H[C(6)]	0.022 (2)	0.063 (8)	−0.252 (12)	5.2 (2.5)
H(1)[C(8)]	0.004 (3)	0.232 (10)	0.007 (13)	7.1 (4.0)
H(2)[C(8)]	0.029 (3)	0.280 (10)	−0.088 (13)	7.6 (4.1)
H(3)[C(8)]	0.019 (2)	0.344 (9)	0.046 (12)	7.5 (3.7)
H(1)[C(9)]	0.022 (3)	0.139 (8)	0.238 (13)	7.8 (3.7)
H(2)[C(9)]	0.026 (3)	0.266 (8)	0.258 (13)	7.9 (4.1)
H(3)[C(9)]	0.054 (2)	0.185 (10)	0.286 (13)	7.9 (3.9)
H(1)[C(10)]	0.071 (2)	0.351 (10)	0.099 (12)	7.0 (3.5)
H(2)[C(10)]	0.082 (3)	0.275 (9)	−0.013 (13)	7.0 (3.8)
H(3)[C(10)]	0.089 (3)	0.246 (7)	0.136 (13)	6.9 (4.5)
H(1)[C(12)]	0.083 (2)	−0.086 (10)	−0.091 (13)	7.2 (3.7)
H(2)[C(12)]	0.056 (2)	−0.152 (8)	−0.018 (13)	7.2 (3.6)
H(3)[C(12)]	0.090 (2)	−0.164 (8)	0.025 (13)	7.3 (3.4)
H(1)[C(13)]	0.067 (2)	−0.128 (9)	0.251 (13)	7.5 (3.4)
H(2)[C(13)]	0.036 (2)	−0.083 (9)	0.198 (12)	7.3 (3.9)
H(3)[C(13)]	0.057 (3)	−0.009 (7)	0.288 (13)	7.5 (4.5)
H(1)[C(14)]	0.112 (3)	0.060 (10)	0.061 (12)	8.0 (3.8)
H(2)[C(14)]	0.115 (3)	−0.026 (10)	0.178 (13)	8.1 (4.5)
H(3)[C(14)]	0.098 (3)	0.085 (9)	0.202 (13)	8.1 (4.0)

[a] The thermal parameters are the form $\exp[-8\pi^2 U(\sin\theta/\lambda)^2]$. [b] The atom H[C($i$)] is the hydrogen atom bonded to the C(i) atom.

uble in aromatic hydrocarbons but insoluble in n-hexane, and stable indefinitely in air.

The mass spectra of PtL_2 (Table IV) show the corresponding parent and fragment ions with a stepwise loss of alkyl substituents of phosphine as olefin with the isotopic pattern expected for platinum metal.

A linear structure for **1, 2, 4,** and **5** is readily deducible from the 1:2:1 triplet[29,30] of the *tert*-butyl proton signal (Table V), and confirmed for **2** and **5** by x-ray analysis (vide infra). The complexes **2** and **5** show similar temperature-dependent ortho-proton NMR spectra suggestive of a restricted rotation of the phenyl rings. Thus two ortho-proton signals of **2** and **5** observed at −70 °C as two broad multiplets (**2,** δ 7.55 and 9.33; **5,** δ 7.40 and 9.38) of an equal intensity coalesce at −20 °C (**2**) and −21 °C (**5**), respectively. Finally they become a single broad multiplet (**2,** δ 8.40; **5,** δ 8.46) at room temperature. Evaluation of energy parameters of the restricted rotation was not attempted because of the broadness resulting from the multispin–spin interactions with the phosphorus atoms and other phenyl protons. Similarly **7** assumes a linear structure as reflected on the 1:3:3:1 quartet pattern of the methyl proton signal of isopropyl groups caused by coincidence of the $J_{H(CH_3)\text{-}H(CH)}$ with one-half of the sum ${}^3J_{H+P} + {}^5J_{H\text{-}P}$ between the methyl protons and phosphorus atoms. A similar 1:3:3:1 pattern of the methyl proton signal is also observed for *trans*-bis(triisopropyl)phosphine complexes, e.g., *trans*-$Pt(H)_2[P(i\text{-}Pr)_3]_2$,[28] *trans*-$PtCl_2[P(i\text{-}Pr)_3]_2$, and *trans*-$PtH(Cl)[P(i\text{-}Pr)_2]_2$.[28]

The solid three-coordinate complex **8** gives the characteristic odor of free $P(i\text{-}Pr)_3$, a symptom of ligand dissociation, and gradually turns red at room temperature. The dissociation takes place more readily in vacuo to afford the two-coordinate complex **7**. The isopropyl proton signals of **8** at room temperature in benzene are broad (Table V), perhaps because of a ligand exchange reaction. Consistent with this is the cryoscopic molecular weight datum of **8** in benzene showing almost complete dissociation of $P(i\text{-}Pr)_3$.

In contrast to the $P(i\text{-}Pr)_3$ complex, the $PPh(t\text{-}Bu)_2$ complex **2** does not afford three coordination even at −80 °C. Thus a 1:1 mixture of **2** and $PPh(t\text{-}Bu)_2$ in toluene-d_8 at −80 °C shows a ^{1}H NMR resonances consisting of **2** and those of free $PPh(t\text{-}Bu)_2$ (t-Bu, δ 1.14(d); ortho-H, δ 7.56).

The three-coordinate phosphite complex **9** does not show any tendency to dissociate or associate to give two or four coordination, respectively. Thus, ^{1}H NMR spectra of a 1:1 or 1:3 mixture of **9** and free $P(O\text{-}o\text{-}C_6H_4CH_3)_3$ in benzene-d_6 at 35 °C shows signals due to **9** (CH_3, δ 2.01(s); meta- and para-H, δ 0.89(m); ortho-H, δ 7.48 (broad d)) and those due to $P(O\text{-}o\text{-}C_6H_4CH_3)_3$ (CH_3, δ 2.14(s); meta- and ortho-H, δ 6.92(m); ortho-H, δ 7.32 (broad d)). The line widths at half height of CH_3 proton signals of **9** and $P(O\text{-}o\text{-}C_6H_4CH_3)_3$ are independent of the concentration of free $P(O\text{-}o\text{-}C_6H_4CH_3)_3$. **9** was recovered quantitatively from the above mixtures. The absence of four-coordinate species $Pt[P(O\text{-}o\text{-}C_6H_4CH_3)_3]_4$ agrees with the cryoscopic molecular weight measurement of **9**. This contrasts to the existence of $Ni[P(O\text{-}o\text{-}C_6H_4CH_3)_3]_4$.[31]

Description of Structure. The crystal structures of the complexes, **2** and **5**, are composed of discrete molecules separated by normal van der Waals' distances (Figure 1), the shortest distance being 2.62 (14) Å between H(2)[C(10)] and H[C(3)] for **2,** and 2.64 (15) Å between H(2)[C(14)] and H(3)[C(12)] for **5.** The disposition of complex molecules in-

Table IV. Mass Spectra of $Pt(PR_3)_2$[a]

Assignment	$Pt[P(t\text{-}Bu)_3]_2$	$Pt[PPh(t\text{-}Bu)_2]_2$	$Pt[P(c\text{-}C_6H_{11})_3]_2$	$Pt[P(i\text{-}Pr)_3]_2$
M^+	599 (43.4)	639 (36.7)	755 (28.8)	515 (74.7)
$[M - (R - 1)]^+$	543 (14.8)	583 (18.6)[b]	673 (66.3)	473 (47.7)
$[M - 2(R - 1)]^+$	487 (88.9)	527 (65.3)[b]	591 (100)	431 (100)
$[M - 3(R - 1)]^+$	431 (100)	471 (100)[b]	509 (75.4)	389 (84.7)
PtP_2^+	257 (23.3)	257 (32.5)	257[c]	257 (19.0)

[a] The relative intensities are shown in the parentheses. [b] R = t-Bu. [c] Too weak to evaluate the relative intensity.

Table V. ^1H NMR Spectra of Two and Three Coordinate Complexes

		Chemical shift (ppm, Me_4Si)[a]	$^3J_{H-P} + ^5J_{H-P}$	Area	Assignment
$Pd[P(t\text{-}Bu)_3]_2$	1	1.51 (t)	12.0		*t*-Bu
$Pd[PPh(t\text{-}Bu)_2]_2$[b]	2	1.48 (t)	12.7	9	*t*-Bu
		8.40 (m)[c]		1	*o*-H
		6.94–7.30 (m)		*d*	*m*- and *p*-H
$Pd[P(c\text{-}C_6H_{11})_3]_2$	3	0.70–2.60 (m)			$c\text{-}C_6H_{11}$
$Pt[P(t\text{-}Bu)_3]_2$	4	1.57 (t)	12.3		*t*-Bu
$Pt[PPh(t\text{-}Bu)_2]_2$[b]	5	1.56 (t)	13.5	9	*t*-Bu
		8.46 (m)[c]		1	*o*-H
		6.90–7.30 (m)		*d*	*m*- and *p*-H
$Pt[P(c\text{-}C_6H_{11})_3]_2$	6	0.70–2.60 (m)			$c\text{-}C_6H_{11}$
$Pt[P(i\text{-}Pr)_3]_2$	7	1.24 (q)[e]	14.0	6	CH_3
		1.96 (m)		1	CH
$Pt[P(i\text{-}Pr)_3]_3$	8	1.24 (b)		6	CH_3
		1.86 (b)		1	CH

[a] Measured in benzene-d_6 at 22.5°. [b] Measured in toluene-d_8 at 22.5 °C. [c] At −71 °C the ortho-proton signal of 2 and 5 is observed at δ 7.55 (m), 9.33 (m) and 7.40 (m), 9.38 (m) in equal intensity, respectively. [d] Owing to the overlap with solvent signal the area cannot be evaluated exactly. [e] A 1:3:3:1 quartet, $J_{H(CH_3)-H(CH)} = 7.0$ Hz.

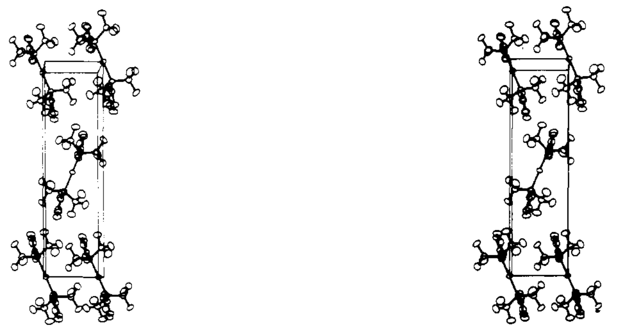

Figure 1. A stereoscopic drawing of the crystal structure of $Pt[PPh(t\text{-}Bu)_2]_2$. The origin of the cell is the upper left corner. The $+c/2$ direction is from the drawing plane toward the viewer, the $+a/2$ direction is from top to bottom, and the $+b/2$ direction is right to origin. The 50% probability vibrational ellipsoids are shown.

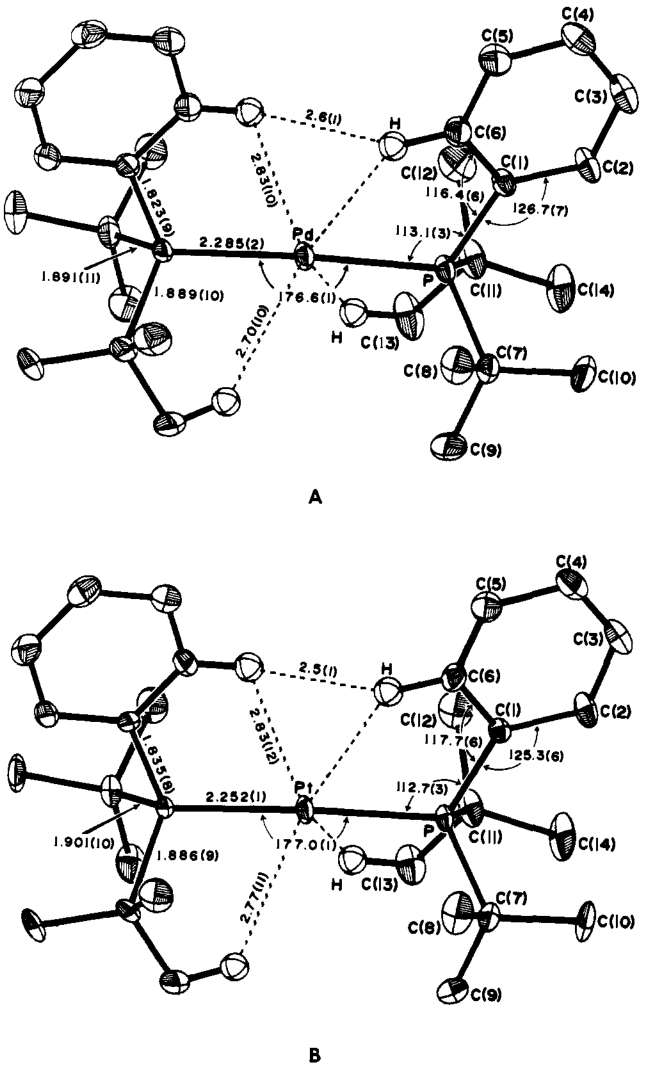

Figure 2. Perspective drawings of the molecules, $Pd[PPh(t\text{-}Bu)_2]_2$ (A) and $Pt[PPh(t\text{-}Bu)_2]_2$ (B). The thermal ellipsoids have been drawn to include 30% of the probability distribution, and for clarity regular hydrogen atoms have been omitted from figures except the two atoms attached to the C(6) and C(13) atoms.

dicated by the thermal ellipsoids is shown in Figure 2, which also indicates the atom numbering scheme. Root-mean-square displacements along the principal axes of the thermal ellipsoid are shown in Table VI. Figure 3 shows the eclipsed conformation of 5 projected along the P–P′ vector. In Table VII are compared selected interatomic distances and angles, and in Table VIII those including the hydrogen atoms.[31]

Both complexes are isostructural having crystallographic C_2 symmetry. The metal atom assumes a slightly bent linear coordination with a P–Pd–P angle of 176.6 (1)° and a P–Pt–P angle of 177.0 (1)°. The normal to the phenyl plane forms an angle of 77.5° with the Pd–P vector. The corresponding angle for 5 is 78.8°. The dihedral angles between the phenyl rings being 3.6° and 3.3° in 2 and 5, respectively.

In each ligand the P–C(Ph) bond length is shorter than the P–C(*t*-Bu) bond length by 0.07 and 0.06 Å for 2 and 5, respectively.

Discussion

The Pt–P distances in Pt(0) complexes[32-42] as far as we know are compared in Table IX. The distances found in the π-acid complexes of formula $Pt(\pi\text{-acid})(PPh_3)_2$ fall within a range of 2.26–2.33 Å. The observed distance 2.252 (1) Å for 5 is shorter than these values suggesting that the M–P distance is not merely governed by the metal effective charge.

An important contribution of $d\pi$–$d\pi$ bonding can be expected for the M–P bond with a strong acceptor PF_3 as in $Pt(PF_3)_4$.[32] Then a question arises as to the nature of the bond with an electron-donating phosphine such as $PPh(t\text{-}Bu)_2$. For the discussion we need to know a reliable covalent radius of Pt(0). In cluster complex $Pt_4(PPhMe_2)_4(CO)_5$,[43] the Pt(0)–Pt(0) bond length, though bridged by a carbonyl group,

Table VI. Root-Mean-Square Displacements along the Principal Axes of the Thermal Ellipsoid (Å)

	$Pd[PPh(t\text{-}Bu)_2]_2$			$Pt[PPh(t\text{-}Bu)_2]_2$		
Atom	Min.	Inter.	Max.	Min.	Inter.	Max.
Metal	0.142	0.201	0.261	0.152	0.175	0.218
P	0.142	0.180	0.248	0.155	0.162	0.213
C(1)	0.169	0.187	0.255	0.142	0.190	0.215
C(2)	0.171	0.218	0.333	0.166	0.200	0.300
C(3)	0.189	0.229	0.353	0.160	0.253	0.332
C(4)	0.183	0.269	0.311	0.183	0.258	0.302
C(5)	0.171	0.248	0.352	0.180	0.263	0.278
C(6)	0.195	0.216	0.287	0.151	0.220	0.275
C(7)	0.175	0.216	0.282	0.190	0.211	0.243
C(8)	0.235	0.250	0.350	0.210	0.245	0.285
C(9)	0.215	0.302	0.353	0.186	0.271	0.342
C(10)	0.187	0.289	0.355	0.165	0.289	0.306
C(11)	0.187	0.213	0.306	0.170	0.202	0.263
C(12)	0.218	0.280	0.335	0.211	0.296	0.306
C(13)	0.190	0.243	0.424	0.163	0.268	0.324
C(14)	0.166	0.271	0.385	0.164	0.247	0.367

Table VII. Selected Interatomic Distances (Å) and Angles (deg)

	$Pd[PPh(t\text{-}Bu)_2]_2$		$Pt[PPh(t\text{-}Bu)_2]_2$	
M-P	2.285 (2)		2.252 (1)	
P-C(1)	1.823 (9)		1.835 (8)	
C(1)-C(2)	1.391 (11)	1.391 (14)	1.415 (11)	1.390 (14)
C(2)-C(3)	1.384 (15)		1.404 (16)	
C(3)-C(4)	1.391 (16)		1.375 (16)	
C(4)-C(5)	1.385 (15)		1.367 (15)	
C(5)-C(6)	1.401 (15)		1.398 (12)	
C(1)-C(6)	1.393 (13)		1.379 (11)	
P-C(7)	1.891 (11)	1.890 (10)	1.901 (10)	1.894 (10)
P-C(11)	1.889 (10)		1.886 (9)	
C(7)-C(8)	1.541 (16)	1.542 (15)	1.531 (16)	1.542 (15)
C(7)-C(9)	1.540 (17)		1.539 (16)	
C(7)-C(10)	1.543 (13)		1.538 (14)	
C(11)-C(12)	1.554 (18)		1.548 (17)	
C(11)-C(13)	1.536 (16)		1.546 (15)	
C(11)-C(14)	1.537 (14)		1.547 (15)	
P-M-P′	176.6 (1)		177.0 (1)	
M-P-C(1)	113.1 (3)		112.7 (3)	
M-P-C(7)	112.9 (3)		112.6 (3)	
M-P-C(11)	109.4 (3)		109.9 (3)	
P-C(1)-C(2)	126.7 (7)		125.3 (6)	
P-C(1)-C(6)	116.4 (6)		117.7 (6)	
P-C(7)-C(8)	104.2 (7)		104.2 (7)	
P-C(7)-C(9)	111.1 (8)		108.5 (7)	
P-C(7)-C(10)	117.2 (7)		116.7 (7)	
P-C(11)-C(12)	104.7 (8)		104.9 (8)	
P-C(11)-C(13)	107.8 (7)		108.1 (7)	
P-C(11)-C(14)	117.6 (8)		119.0 (7)	
C(1)-C(2)-C(3)	121.2 (9)	120.0 (9)	120.4 (8)	120.0 (9)
C(2)-C(3)-C(4)	121.6 (9)		120.1 (9)	
C(3)-C(4)-C(5)	117.9 (9)		120.5 (10)	
C(4)-C(5)-C(6)	120.3 (9)		119.4 (10)	
C(5)-C(6)-C(1)	121.9 (8)		122.5 (8)	
C(6)-C(1)-C(2)	117.0 (9)		116.9 (7)	
C(7)-P-C(1)	105.3 (4)		104.2 (4)	
C(1)-P-C(11)	104.3 (4)		105.0 (4)	
C(7)-P-C(11)	111.6 (5)		112.3 (4)	

Table VIII. Interatomic Distances (Å) and Angles (deg) Including the Hydrogen Atoms

	$Pd[PPh(t\text{-}Bu)_2]_2$	$Pt[PPh(t\text{-}Bu)_2]_2$
(i) Nonbonded Interatomic Distances		
M···H[C(6)]	2.83 (10)	2.83 (12)
M···H(1)[C(8)]	2.97 (8)	2.93 (13)
M···H(2)[C(13)]	2.70 (10)	2.77 (11)
(ii) Phenyl Group		
(a) Bond Distances		
C(2)-H	0.97 (9)	0.97 (10)
C(3)-H	0.98 (10)	1.00 (10)
C(4)-H	0.98 (10)	0.98 (13)
C(5)-H	0.98 (10)	1.00 (11)
C(6)-H	0.98 (9)	0.97 (9)
Mean	0.98 (10)	0.98 (11)
(b) Mean Bond Angle		
H-C···C	120 (6)	120 (6)
(iii) *t*-Bu Groups		
(a) Bond Distances		
C(8)-H(1)	1.01 (9)	1.00 (10)
C(8)-H(2)	0.94 (9)	0.97 (10)
C(8)-H(3)	0.95 (9)	1.02 (10)
Mean	0.97 (9)	1.00 (10)
C(9)-H(1)	0.98 (10)	0.99 (11)
C(9)-H(2)	0.96 (10)	0.96 (11)
C(9)-H(3)	0.99 (7)	1.03 (12)
Mean	0.98 (9)	0.99 (11)
C(10)-H(1)	1.04 (10)	1.03 (12)
C(10)-H(2)	0.98 (9)	0.95 (13)
C(10)-H(3)	1.02 (10)	0.95 (13)
Mean	1.01 (10)	0.98 (13)
C(12)-H(1)	0.98 (9)	0.96 (13)
C(12)-H(2)	0.99 (9)	1.05 (11)
C(12)-H(3)	1.02 (10)	0.95 (11)
Mean	1.00 (9)	0.99 (11)
C(13)-H(1)	1.02 (10)	0.98 (11)
C(13)-H(2)	1.01 (10)	0.98 (11)
C(13)-H(3)	0.94 (9)	1.00 (11)
Mean	0.99 (10)	0.99 (11)
C(14)-H(1)	0.98 (10)	0.96 (12)
C(14)-H(2)	0.94 (10)	0.93 (14)
C(14)-H(3)	0.97 (10)	1.05 (12)
Mean	0.96 (10)	0.99 (13)
(b) Mean Bond Angles		
H-C(8)-H	108 (8)	110 (10)
H-C(9)-H	108 (7)	109 (10)
H-C(10)-H	109 (7)	108 (10)
H-C(12)-H	110 (8)	109 (10)
H-C(13)-H	109 (8)	109 (10)
H-C(14)-H	108 (8)	108 (11)
H-C(8)-C(7)	111 (6)	109 (8)
H-C(9)-C(7)	110 (6)	110 (8)
H-C(10)-C(7)	110 (5)	110 (7)
H-C(12)-C(11)	109 (5)	109 (7)
H-C(13)-C(11)	109 (6)	110 (7)
H-C(14)-C(11)	111 (6)	110 (8)

is 2.76 Å. A reasonable covalent radius of Pt(0), we believe, would thus be no less than 1.38 Å. Accepting this value and 1.10 Å for the covalent radius of the P atom,[44] we find that the distance 2.252 Å for **5** is much shorter than the sum of these covalent radii. Hence it seems reasonable to assume a simultaneous contribution of both σ- and π-bonding, a synergic interaction. Interestingly, the distance of 2.290 Å found in $Pt(O_2)[PPh(t\text{-}Bu)_2]_2$,[42] containing the strongest π-acid O_2 (electron affinity, 0.85 eV[45]), is longer than the value 2.252 Å for **5**. If the bond strength is mainly governed by the σ-donor–acceptor type bonding, then the M-P bond in the dioxygen complex should be stronger than the two-coordinate complex **5**. One might seek then a rationale in contribution of the M-P π back-bonding. However, in view of the feeble dπ-accepting character of $PPh(t\text{-}Bu)_2$ we expect less contribution of the dπ-pπ bonding compared to the σ-bonding. A more reasonable rationale may be found in the change of a covalent radius of a metal susceptible to the change in hybridization.[46] This view receives support from the relative Pt-P distances for the three-coordinate $Pt(PPh_3)_3$[34] and the four-coordinate complex

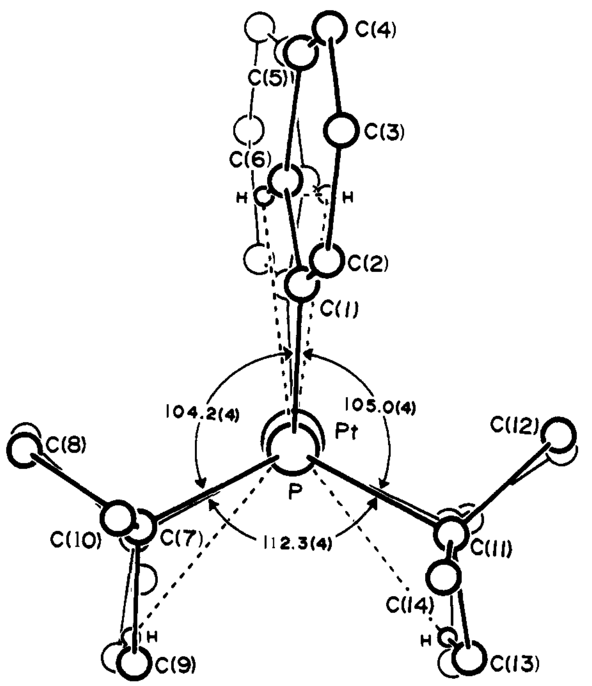

Figure 3. A drawing of the eclipsed comformation of Pt[PPh(t-Bu)$_2$]$_2$ projected along the P-P′ vector.

Table IX. Pt-P Bond Distances of Pt(0) Complexes

Pt-P (Å)	Complexes	Ref
2.240 (10)	Pt(PF$_3$)$_4$	32
2.334 (7), 2.352 (8)	Pt(CO)(PPh$_3$)$_3$	33
2.25 (1), 2.28 (1)	Pt(PPh$_3$)$_3$	34
2.252 (1)	Pt[PPh(t-Bu)$_2$]$_2$ (**5**)	This work
2.264 (1), 2.271 (1)	Pt(cyclohexyne)(PPh$_3$)$_2$	35
2.264 (1), 2.270 (1)	Pt(cycloheptyne)(PPh$_3$)$_2$	35
2.277 (1), 2.285 (1)	Pt(CF$_3$C≡CCF$_3$)(PPh$_3$)$_2$	36
2.261 (4), 2.298 (4)	Pt(CH$_2$=C=CH$_2$)(PPh$_3$)$_2$	37
2.29	Pt($\Delta^{1,4}$-bicyclo[2.2.0]-hexene)(PPh$_3$)$_2$	38
2.278 (8), 2.292 (7)	Pt(CCl$_2$=CCl$_2$)(PPh$_3$)$_2$	39
2.303 (6), 2314 (5)	Pt(CCl$_2$=CF$_2$)(PPh$_3$)$_2$	39
2.260 (6), 2.339 (6)	Pt[C(CN)$_2$=CCl$_2$](PPh$_3$)$_2$	40
2.291 (9), 2.288 (8)	Pt(TCNE)(PPh$_3$)$_2$	41
2.290 (4)	Pt(O$_2$)[PPh(t-Bu)$_2$]$_2$	42

Pt(CO)(PPh$_3$)$_3$[33] containing CO, a ligand of stronger acceptor than PPh$_3$. The shorter Pt-P distance of **5** compared with Pt(PPh$_3$)$_3$[34] may be similarly understood.

The covalent radius of Pd(0) is also unavailable. From the comparable metallic radii[47] (1.375 Å for Pd and 1.387 Å for Pt) and divalent radii[44,48] (1.31 Å for Pd(II) and 1.31 Å for Pt(II)), we should assume a similar value for both metals. A reasonable value of 1.35 Å was assessed from the binuclear complex Pd$_2$(C$_3$H$_5$)(PPh$_3$)$_2$.[49] Thus the significantly longer Pd-P distance of **2** (2.285 (2) Å) compared with a Pt-P distance of **5** may be ascribed to the difference in M-P bond strengths.

The above discussion, however, neglects steric effects of the phosphine substituents which may affect the M-P bond length. The substituent angles C(R)-P-C(R) around a P atom coordinated to a metal generally exhibit a slight deviation from the ideal tetrahedral angle (109.5°). The values range from 100 to 107° as found in triphenylphosphine complexes[33,35,50] and Pt(B$_3$H$_7$)(PPhMe$_2$)$_2$.[51] With bulky substituents the angle naturally increases. In fact, C(t-Bu)-P-C(t-Bu) and C(t-Bu)-P-(Ph) for **2** are 111.6 and 104.3°, respectively, while the corresponding values for **5** are 112.3 and 105.0°. It can be expected that the bulkier the R group, the larger the R-P-R angle. The distortion should destabilize the sp^3 hybridization at the P atom. A systematic variation of substituent bulkiness is required to assess this subtle effect on the M-P bond strengths.

The most remarkable structural feature of **2** and **5** is that substituents of the phosphorus atoms form an eclipsed conformation with the nearly parallel phenyl planes. A rationale may be found in the proximity of two ortho-hydrogen atoms of the phenyl groups, 0.98 (10) and 0.97 (9) Å for C(6)-H distances in **2** and **5**, respectively. Accepting that the C-H distances in x-ray analysis are systematically underestimated by ca. 0.10-0.15 Å,[52] the true C(6)-H distance may be assessed as 1.05-1.10 Å for **2** and 1.07-1.12 Å for **5**, in agreement with the well established value of 1.10 Å by spectroscopic methods.[53] If the C-H bond distance is so corrected along the C-H direction found in the present study, the distance will increase to 1.10 Å, resulting in the Pd···H and Pt···H distances of 2.83 Å. These distances are comparable to the estimated metal···ortho-hydrogen distances in PdI$_2$(PPhMe$_2$)$_2$[54] (2.84-2.85 Å) and significantly short in comparison with those in Pt(PPh$_3$)$_3$[34] (3.2 Å). A very short distance of 2.59 Å was reported for RuH(Cl)(PPh$_3$)$_2$.[55] The distance between the two ortho-hydrogen atoms can be estimated to be ca. 2.6 Å in **2** and ca. 2.5 Å in **5**. These values roughly correspond to the sum of the van der Waals' radius of the H atom.[44] An attraction between the two hydrogen atoms may exist,[56] since a repulsive interaction between the atoms, if it exists, would easily be removed by rotations around the P-metal bonds and of the P-aromatic carbon bond as well. The molecular model does not indicate any steric compression between the phosphorus substituents preventing the staggering. The attractive force, accounting for the eclipsed conformation, appears to be manifested by the distortion of angles P-C(1)-C(6) (average,

Table X. Relation between Cone Angle of L and Coordination Number of ML$_n$ (M = Pd, Pt), and Compressibility of Cone Angle

Ligand	Cone angle (deg)	n found	Cone angle found
P(t-Bu)$_3$	182 ± 2	2	103^a in RhH$_2$Cl[P(t-Bu)$_3$]$_2$[42]
PPh(t-Bu)$_2$	170 ± 2	2	100^b in $trans$-MHCl[PPh(t-Bu)$_2$]$_2$[27] (M = Pd, Pt)
P(c-C$_6$H$_{11}$)$_3$	179 ± 10	2	120^c in Ni[P(c-C$_6$H$_{11}$)$_3$]$_3$
P(O-o-C$_6$H$_4$CH$_3$)$_3$	141,^{d} 160 ± 10	3	109^c in Ni[P(O-o-C$_6$H$_4$CH$_3$)$_3$]$_4$[30]
P(i-Pr)$_3$	160 ± 10	2, 3	120^c in Pt[P(i-Pr)$_3$]$_3$
PPh$_3$	145 ± 2	3, 4	109^c in Pt(PPh$_3$)$_4$
PEt$_3$	132 ± 4	3, 4	

[a] Evaluated based on the molecular parameters. [b] Estimated assuming M-H and M-Cl bond lengths to be 1.65 and 2.3 Å, respectively. [c] Formally valency angle; however, may be equivalent to cone angle. [d] In view of the nonexistence of tetracoordinate complex PtL$_4$ (L = P(O-o-C$_6$H$_4$CH$_3$)$_3$), the revised cone angle for P(O-o-C$_6$H$_4$CH$_3$)$_3$ seems too small since PtL$_4$ exists with PPh$_3$ of which cone angle was estimated to be 145 ± 2°.

Table XI. Energy Level of Atomic Orbitals[62]

	Ni(0)	Pd(0)	Pt(0)
d–s (eV)[a]	−1.80	0.81	−0.76
s–p (eV)[b]	3.52	3.42	4.04

[a] $d^{10}(^1S_0) \rightarrow d^9s(^3D_3)$; the term of d^9s for Pt(0) has not been determined yet. [b] $d^9s(^3D_3) \rightarrow d^9p(^3P_2)$.

117.0°) and P–C(1)–C(2) (average, 126.0°). The geometry around the metal also suggests involvement of the metal atom in attractive interaction.[9] The attraction is apparently retained in solution at low temperature as shown by the enormous deshielding (δ 9.33 for **2** and 9.38 for **5**) observed for the proximal ortho-hydrogen atoms.

Short M···H distances are also observed for some *tert*-butyl hydrogen atoms; the corrected values for Pd···H[C(13)] and Pd···H[C(8)] in **2** are 2.70 and 2.97 Å, respectively, while the corresponding values for **5** are 2.77 and 2.93 Å. These distances also suggest van der Waals' contact of the aliphatic hydrogen atoms to the metal. These proximal hydrogen atoms of $PPh(t\text{-}Bu)_2$ apparently prevent approach of solvent molecules, contributing to their kinetic stability in solution.

As shown in Table X, the coordination number of ML_n is primarily governed by the steric nature of the ligand. A measure for steric bulk may be Tolman's cone angle.[57] Many complexes isolated, however, indicate considerable compressibility of the angle. From the x-ray structure of $RhH_2Cl[P(t\text{-}Bu)_3]_2$,[42] which assumes a distorted trigonal bipyramidal configuration with a bent P–Rh–P bond, we assessed the cone angle of $P(t\text{-}Bu)_3$ to be about 103°, a little more than 40% reduction in the angle. Similar reduction is seen for $PPh(t\text{-}Bu)_2$, $P(c\text{-}C_6H_{11})_3$, $P(O\text{-}o\text{-}C_6H_4CH_3)_3$, etc. (Table X).

Let us now examine factors determining the preferred coordination number. $P(i\text{-}Pr)_3$ and $P(O\text{-}o\text{-}C_6H_4CH_3)_3$ differ considerably in electronic property but the steric requirements may not differ significantly. The strong propensity of $Pt[P(i\text{-}Pr)_3]_3$ to dissociate 1 mol of ligand in the solid state and in solution contrasts to the reluctance of $Pt[P(O\text{-}o\text{-}C_6H_4CH_3)_3]_3$ to undergo dissociation implying the importance of the electronic property of the ligand. Ni(0) forms NiL_4 with $P(O\text{-}o\text{-}C_6H_4CH_3)_3$[30] whereas Pt(0) with this phosphite gives PtL_3 which shows no indication to form PtL_4 in solution. Similarly with $P(c\text{-}C_6H_{11})_3$, the existence of stable PtL_2 contrasts to the formation of NiL_3.[8] Here the electronic property of metal atoms is operating. Apparently Ni(0) tends to assume a higher coordination number compared to Pd(0) or Pt(0); a similar trend has long been known for the group 1b triad, Cu(I), Ag(I), and Au(I).[58] The trend may be accounted for by the $d\pi$-donating property which falls in a sequence Ni > Pt > Pd, a sequence in parallel with the promotional energy $d^{10} \rightarrow d^9p^1$; 1.72, 4.23, and 3.28 eV for Ni, Pd, and Pt, respectively.

The preceding argument is based on Pauling's electroneutrality principle.[59,60] The preferred two coordination of Pt(0) with the electron donating $P(i\text{-}Pr)_3$ rather than with a more electron accepting ligand is also explicable by this principle. Orgel[61] has ascribed the propensity of d^{10} ion to form low-coordination to the nd–$(n + 1)$s energy separation, while Nyholm[58] considered the $(n + 1)$s–$(n + 1)$p separation more important on the basis of the hybridization scheme. The two interpretations perhaps stand on the same theoretical ground, and, more importantly, the interpretations would be valid only when a constant metal–ligand atom distance is assumed. Since this assumption will not hold even for a series of complexes of the same coordination number, the lack of apparent correlation between the preferred coordination number and the energy separation (Table XI) is not surprizing. For the judicious discussion, we require a further array of x-ray data for these low-valent low-coordination complexes.

Supplementary Material Available: Structure factors (19 pages). Ordering information is given on any current masthead page.

References and Notes

(1) (a) Osaka University. (b) Kwansei Gakuin University.
(2) R. Ugo, *Coord. Chem. Rev.*, **3**, 319 (1968).
(3) J. Halpern and T. A. Weil, *J. Chem. Soc., Chem. Commun.*, 631 (1973), and references therein.
(4) R. Ugo, G. LaMonica, F. Cariati, S. Cerini, and F. Conti, *Inorg. Chim. Acta*, **4**, 390 (1970).
(5) (a) D. M. Blake and C. J. Nyman, *J. Am. Chem. Soc.*, **92**, 5359 (1970); (b) D. M. Blake and R. Mersecchi, *J. Chem. Soc. D*, 1045 (1971).
(6) S. Otsuka, K. Tani, I. Kato, and O. Teranaka, *J. Chem. Soc., Dalton Trans.*, 2216 (1974).
(7) E. Englert, P. W. Jolly, and G. Wilke, *Angew. Chem.*, **83**, 84 (1971).
(8) P. W. Jolly, K. Jonas, C. Krüger, and Y. H. Tsay, *J. Organomet. Chem.*, **33**, 109 (1971).
(9) M. Matsumoto, H. Yoshioka, K. Nakatsu, T. Yoshida, and S. Otsuka, *J. Am. Chem. Soc.*, **96**, 3322 (1974).
(10) A. Musuco, W. Kuran, A. Silvani, and M. W. Anker, *J. Chem. Soc., Chem. Commun.*, 938 (1973).
(11) A. Immirzi and A. Musco, *J. Chem. Soc., Chem. Commun.*, 400 (1974).
(12) K. Kudo, M. Hidai, and Y. Uchida, *J. Organomet. Chem.*, **56**, 413 (1973).
(13) R. van der Linde and R. O. der Jongh, *J. Chem. Soc. D*, 563 (1971).
(14) S. Otsuka and T. Yoshida, "Proceedings of the 16th International Conference on Coordination Chemistry", 236a (1974).
(15) M. Green, J. A. Howard, J. L. Spencer, and F. G. A. Stone, *J. Chem. Soc., Chem. Commun.*, 3 (1975).
(16) H. Brüger and U. Wanagat, *Monatsh. Chem.*, **94**, 1007 (1963).
(17) H. Brüger and U. Wanagat, *Monatsh. Chem.*, **95**, 1099 (1964).
(18) H. Hofmann and P. Schellenbeck, *Chem. Ber.*, **100**, 692 (1967).
(19) B. E. Mann, B. L. Shaw, and R. M. Slade, *J. Chem. Soc. A*, 2976 (1971).
(20) K. Issleib and A. Brack, *Z. Anorg. Allg. Chem.*, **277**, 258 (1954).
(21) A. H. Cowley and M. W. Taylor, *J. Am. Chem. Soc.*, **91**, 2915 (1969).
(22) E. N. Walsh, *J. Am. Chem. Soc.*, **81**, 3023 (1959).
(23) B. L. Shaw, *Proc. Chem. Soc., London*, 247 (1960).
(24) D. T. Cromer and J. T. Waber, *Acta Crystallogr.*, **18**, 104 (1965).
(25) R. F. Stewart, E. R. Davidson, and W. T. Simpson, *J. Chem. Phys.*, **42**, 3175 (1965).
(26) D. T. Cromer and D. Liberman, *J. Chem. Phys.*, **53**, 1891 (1970).
(27) See paragraph at the end of the paper regarding supplementary material.
(28) S. Otsuka and T. Yoshida, to be submitted for publication.
(29) R. K. Harris, *Can. J. Chem.*, **42**, 2275 (1964).
(30) A. Pidcock and J. F. Nixon, *Annu. Rev. NMR Spectrosc.* **2**, 345 (1969).
(31) L. W. Grosser and C. A. Tolman, *Inorg Chem.*, **9**, 2350 (1970).
(32) J. C. Marriott, J. A. Salthouse, M. J. Ware, and J. M. Freeman, *Chem. Commun.*, 593 (1970).
(33) V. G. Albano, G. M. B. Ricci, and P. L. Bellon, *Inorg. Chem.*, **10**, 2109 (1969).
(34) V. Albano, P. L. Bellon, and V. Scatturin, *Chem. Commun.*, 507 (1966).
(35) G. B. Robertson and P. O. Whimp, *J. Am. Chem. Soc.*, **97**, 1051 (1975).
(36) B. W. Davis and N. C. Payne, *Inorg. Chem.*, **13**, 1848 (1974).
(37) K. Okamoto, Y. Kai, N. Yasuoka, and N. Kasai, *J. Organomet. Chem.*, **65**, 427 (1974).
(38) M. E. John, J. A. McGinnety, and K. B. Wibert, *J. Am. Chem. Soc.*, **96**, 6531 (1974).
(39) J. N. Francis, A. McAdam, and J. A. Ibers, *J. Organomet. Chem.*, **29**, 131 (1971).
(40) J. N. Francis, A. McAdam, and J. A. Ibers, *J. Organomet. Chem.*, **29**, 149 (1971).
(41) G. Bombieri, E. Forsellini, C. Panattoni, R. Graziani, and G. Bandoli, *J. Chem. Soc. A*, 1313 (1970).
(42) K. Nakatsu, private communication.
(43) R. G. Vranka, L. F. Dahl, P. Chini, and J. Chatt, *J. Am. Chem. Soc.*, **91**, 1574 (1969).
(44) L. Pauling, "The Nature of the Chemical Bond", 3d ed, Cornell University Press, Ithaca, N.Y., 1960.
(45) V. I. Vedeneyev, "Bond Energies, Ionization Potentials and Electron Affinities", Arnold, London, 1966, p 195.
(46) R. Mason, *Chem. Soc. Rev.*, **1**, 431 (1972).
(47) L. E. Sutton, *Chem. Soc., Spec. Publ.*, **No. 11** (1958) and **18** (1965).
(48) J. D. Bell, D. Hall, and T. N. Waters, *Acta Crystallogr.*, **21**, 44 (1966).
(49) Y. Kobayashi, Y. Iitaka, and H. Yamazaki, *Acta Crystallogr., Sect. B*, **28**, 899 (1972).
(50) M. R. Churchill and T. A. O'Brien, *J. Chem. Soc. A*, 2970 (1968), and references therein.
(51) L. J. Guggenberger, A. R. Kane, and E. L. Muetterties, *J. Am. Chem. Soc.*, **94**, 5665 (1972).
(52) J. C. Hanson, L. C. Sieker, and L. H. Jensen, *Acta Crystallogr., Sect. B*, **29**, 797 (1973).
(53) "Tables of Interatomic Distances and Configuration in Molecules and Ions", the Chemical Society Press, London, 1958, p 16.
(54) N. A. Bailey and R. Mason, *J. Chem. Soc. A*, 2594 (1968).
(55) S. J. Laplaca and J. A. Ibers, *Inorg. Chem.*, **4**, 778 (1965).
(56) E. L. Eliel, N. L. Allinger, S. J. Angyal, and G. A. Morrison, "Conformational Analysis", Interscience, New York, N.Y., 1965, p 433.
(57) (a) C. A. Tolman, *J. Am. Chem. Soc.*, **92**, 2956 (1970); (b) C. A. Tolman, W. C. Seidel, and L. W. Grossen, *J. Am. Chem. Soc.*, **96**, 53 (1974).

(58) R. S. Nyholm, *Proc. Chem. Soc., London*, 273 (1961).
(59) L. Pauling, *J. Chem. Soc.*, 1461 (1948).
(60) R. S. Nyholm, "Proceedings of the Third International Congress on Catalysis", Vol. 1, North-Holland Publishing Co., Amsterdam, 1965, p 25.
(61) L. E. Orgel, "An Introduction to Ligand Field Theory", Wiley, New York, N.Y., 1960, p 66.
(62) C. Moore, *Nat. Bur. Stand. (U.S.), Cir.*, **No. 467**, Vol. II (1952); Vol. III (1958).

Circularly Polarized Emission Studies on the Chiral Nuclear Magnetic Resonance Lanthanide Shift Reagent Tris(3-trifluoroacetyl-*d*-camphorato)europium(III)

Harry G. Brittain and F. S. Richardson*

Contribution from the Department of Chemistry, University of Virginia, Charlottesville, Virginia 22901.
Received January 19, 1976

Abstract: Total emission (TE) and circularly polarized emission (CPE) spectra are reported for the optically active rare earth chelate system, tris(3-trifluoroacetyl-*d*-camphorato)europium(III) or Eu(facam)$_3$, in powder form at liquid nitrogen temperature and in a variety of pure solvent and mixed solvent systems at room temperature. The detailed features of the TE and CPE spectra are related to structural characteristics of the chelate system and to the nature of chelate:solvent interactions. The emission anisotropy factor, g_{em}, is found to be an especially sensitive probe for studying chelate:solvent adduct formation and for deducing information about the relative coordinative strengths of various solvent molecules which possess nucleophilic donor moieties.

I. Introduction

The spectroscopic and structural properties of lanthanide β-diketonate complexes have been studied extensively over the past 15 years. Many of the earlier spectroscopic studies were stimulated by the potential of these systems as possible lasing materials in solution media. Weissman[1] first reported that certain rare earth chelates, when irradiated by ultraviolet radiation, emit visible light characteristic of the metal ion. The first systematic studies and interpretation of the mechanism of this process were provided by Crosby and co-workers.[2,3] Since these early investigations, a great many additional studies have been reported on the luminescence properties of rare earth chelates both in solution media and in the solid state.[4]

Hinckley[5] first demonstrated (in 1969) the potential application of paramagnetic tris(β-diketonato)lanthanide(III) complexes for inducing shifts in NMR spectra and, since that time, research activity in this area has grown prodigeously.[6] Lanthanide induced shift reagents, or lanthanide shift reagents (LSR), are now used routinely to enhance spectral resolution and clarification of the NMR spectra obtained for functional organic substrate molecules. Additionally, some success has been achieved in using observed lanthanide induced shifts (LIS) to deduce quantitative or semiquantitative structural information about substrate molecules in solution. Crucial to the eventual widespread acceptance and utility of this latter application of LSRs is an understanding or knowledge of: (1) LSR structure in solution in a variety of solvent systems (neat *and* mixed); (2) the stoichiometric and stereochemical characteristics of LSR:substrate binding as a function of various solution conditions (such as solvent, concentration ratios, temperature, etc.); and (3) the detailed nature of the magnetic interactions between the paramagnetic LSR and diamagnetic substrate molecules.

Little is known about the detailed structural characteristics of LSR complexes in solution. In the solid state these complexes are known to form dimers or oligomers, and it is quite possible that in solution at the concentrations normally used in NMR experiments (on the order of 0.5 M), these dimeric or oligomeric species also predominate or exist in significant amounts. The stoichiometries of various LSR:substrate systems under various conditions are, perhaps, better characterized and understood, but the symmetries and coordination geometries of these complexes in solution have not been well characterized. In using LIS data to deduce structural information, it is usually assumed that the LSR:substrate complexes possess axial symmetry (about an axis which includes the lanthanide metal ion and the donor atom(s) of the substrate molecules(s)). This assumption of axial symmetry simplifies enormously the quantitative treatment of the LIS data and its use in making spectra-structure correlations; however, a static axis of symmetry would in most cases not be expected from what structural information does exist on adducts of lanthanide tris(β-diketonate) compounds.[7-9]

In the present study we examine the total emission (TE) and circularly polarized emission (CPE) spectra of the optically active rare earth chelate system, tris(3-trifluoroacetyl-*d*-camphorato)europium(III), in a variety of solvents. Earlier studies in our laboratory have shown CPE (and TE) to be an extremely sensitive technique for probing the structure and structural changes of chiral lanthanide ion complexes in solution.[10-13] This technique combines the structural and stereochemical sensitivity of chiroptical spectroscopy with the instrumental sensitivity of emission spectroscopy.

Tris(3-trifluoroacetyl-*d*-camphorato)europium(III), or Eu(facam)$_3$, is just one member of a series of chiral lanthanide shift reagents which have been used for direct determination of enantiomeric composition and purity by NMR.[14] In the presence of these optically active chelates, enantiomers (that respond to LSRs) generally have nonequivalent NMR spectra. The crystal structure of the dimethylformamide (DMF) adduct of Pr(facam)$_3$ has just recently been reported.[9] In crystalline form this complex was found to exist as a dimer, (facam)$_3$Pr(DMF)$_3$Pr(facam)$_3$, with the DMF oxygen atoms forming bridges between the two Pr(facam)$_3$ moieties. Each Pr atom is nine-coordinate with the oxygen donor atoms occupying the vertices of a distorted monocapped square anti-